

Supporting Information for  
**Two-dimensional Mo<sub>3</sub>(C<sub>6</sub>O<sub>6</sub>)<sub>2</sub> exhibits high activity and selectivity as a catalyst for CO<sub>2</sub> reduction reactions**

Weixiang Geng,<sup>†</sup> Tianchun Li,<sup>†</sup> Xiaorong Zhu,<sup>§</sup> Yu Jing<sup>\*,†</sup>

<sup>†</sup>Jiangsu Co-Innovation Centre of Efficient Processing and Utilization of Forest Resources, College of Chemical Engineering, Nanjing Forestry University, Nanjing 210037, China

<sup>§</sup> School of Chemistry and Chemical Engineering, Nantong University, 226019, China

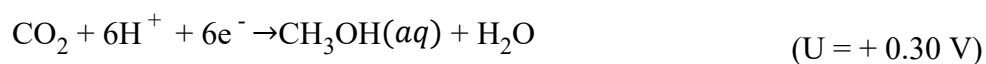
To whom correspondence should be addressed. Email: [yujing@njfu.edu.cn](mailto:yujing@njfu.edu.cn)(YJ)

The number of pages: 4 (S1-S6)

The number of Figures: 3 (Figures S1-S5)

The number of Tables: 1 (Tables S1)

The chemical reduction of CO<sub>2</sub> is a multi-step reaction process, usually involving 2, 6, 8 or 12 electron reaction pathways. The thermodynamically determined equilibrium potentials ( $U_0$ ) for CO<sub>2</sub> reduction to several most common products are listed below:



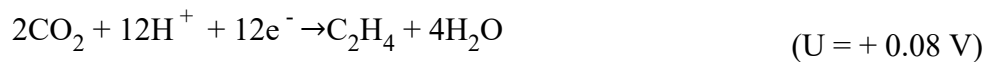


**Table. S1** DFT total energies ( $E_{\text{total}}$ ), zero-point energies (zpe), entropies ( $T^*S$ ) multiplied by temperature ( $T = 298.15\text{K}$ ), and free energies( $G$ ) of gas molecules.

	$E_{\text{total}}$ (eV)	zpe (eV)	$T^*S$	$G$ (eV)
$\text{H}_2$	-6.77	0.27	0.41	-6.91
$\text{H}_2\text{O}$	-14.22	0.56	0.67	-14.33
$\text{CO}_2$	-22.95	0.31	0.66	-23.30

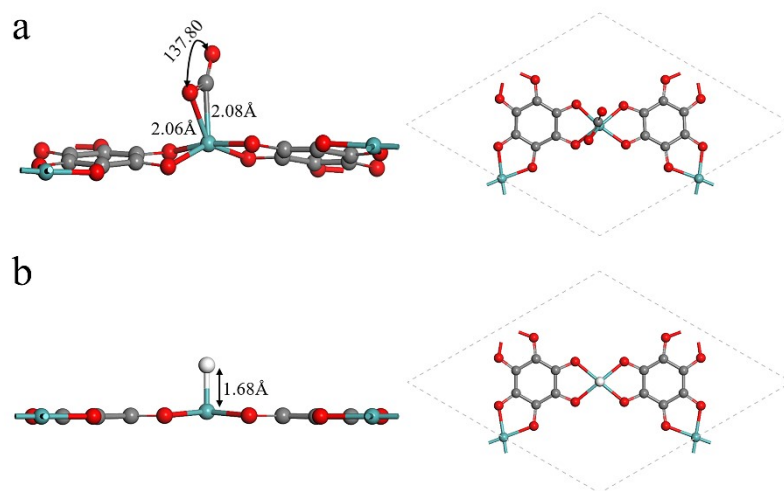


**Fig. S1** The side and top views of  $\text{CO}_2$  (a) and  $^*\text{H}$  (b) adsorbed on  $\text{Mo}_3(\text{C}_6\text{O}_6)_2$ . The colors of H, C, and O atoms are white, gray, and red, respectively.

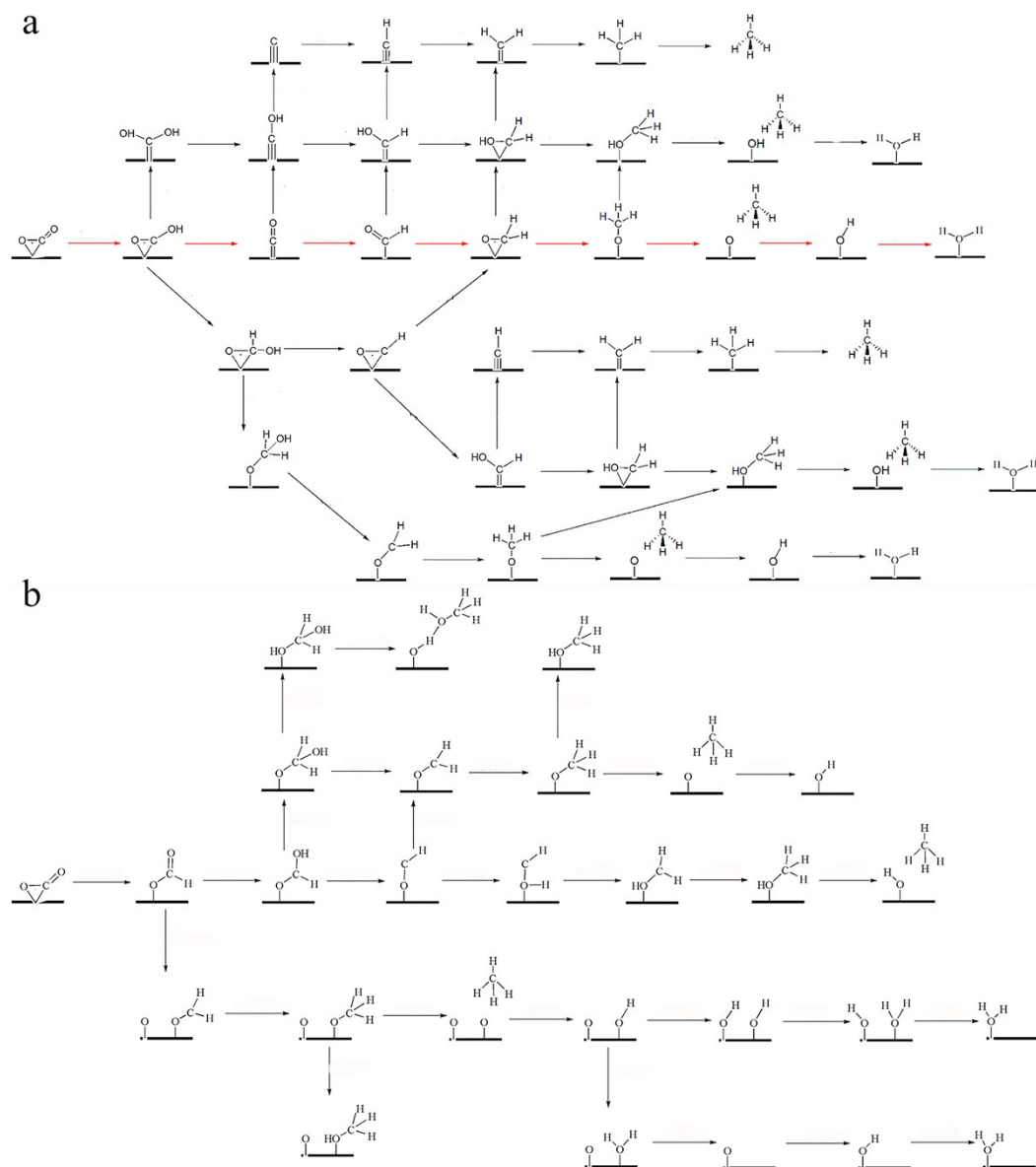


**Fig. S2** Reaction pathways in the (a) “COOH” path and (b) the “OCHO” path. The optimal path is indicated in red arrows.

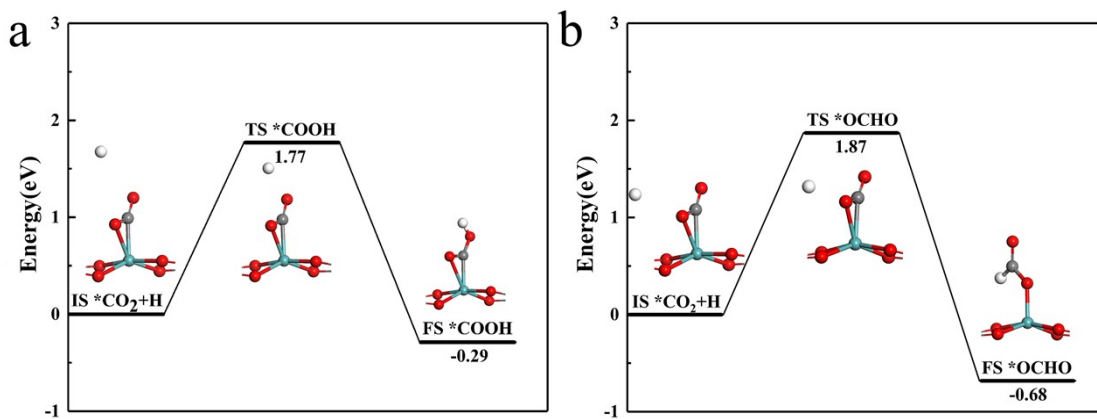


**Fig. S3** Energy profiles for the formed \*COOH(a) and \*OCHO(b) intermediates by the initial hydrogenation of carbon dioxide at  $\text{Mo}_3(\text{C}_6\text{O}_6)_2$ . The structure of each state is given. The \*H and O/C atomic distances in each step are given.

To investigate the most stable surface conformation of  $\text{Mo}_3(\text{C}_6\text{O}_6)_2$  under working conditions. We have plotted Pourbaix diagrams based on thermodynamic data. As shown in Fig. S1, the surface of 2D  $\text{Mo}_3(\text{C}_6\text{O}_6)_2$  is completely covered by \*OH species when the electrode potential is 0 V, independent of the pH value. When an electrode potential of -0.28 V was applied, OH started to be reduced, and the OH coverage on the material surface was 1/3 ML when at the operating potential of CRR. This proves the presence of stable Mo active sites on the MOF surface at the working potential. At an applied potential of -0.90 V, all OH on the  $\text{Mo}_3(\text{C}_6\text{O}_6)_2$  surface is hydrogenated.

Since the working potential of  $\text{Mo}_3(\text{C}_6\text{O}_6)_2$  monolayer catalyzed CRR is -0.58 V at pH = 0 when less than 1/3 of the active sites on the surface are occupied by \*OH, we further considered the effect of axial \*OH ligands on  $\text{Mo}_3(\text{C}_6\text{O}_6)_2$  monolayer to catalyze CRR. The subsequent calculations showed that  $\text{Mo}_3(\text{C}_6\text{O}_6)_2$ -OH can catalyze the reduction of  $\text{CO}_2$  to  $\text{CH}_4$  at a limiting potential of -0.39 V, and according to the Pourbaix diagram there is a large amount of \*OH ligands present on the  $\text{Mo}_3(\text{C}_6\text{O}_6)_2$  surface at this limiting potential, indicating the good stability of the material during the reaction.

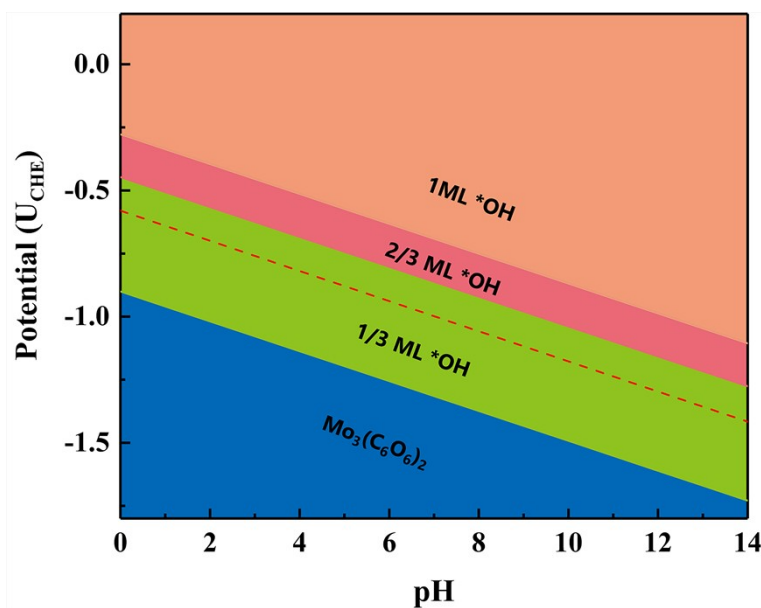


**Fig. S4** Pourbaix diagram for the  $\text{Mo}_3(\text{C}_6\text{O}_6)_2$  system. The red dashed line represents the limiting potential of  $\text{CH}_4$  formation.

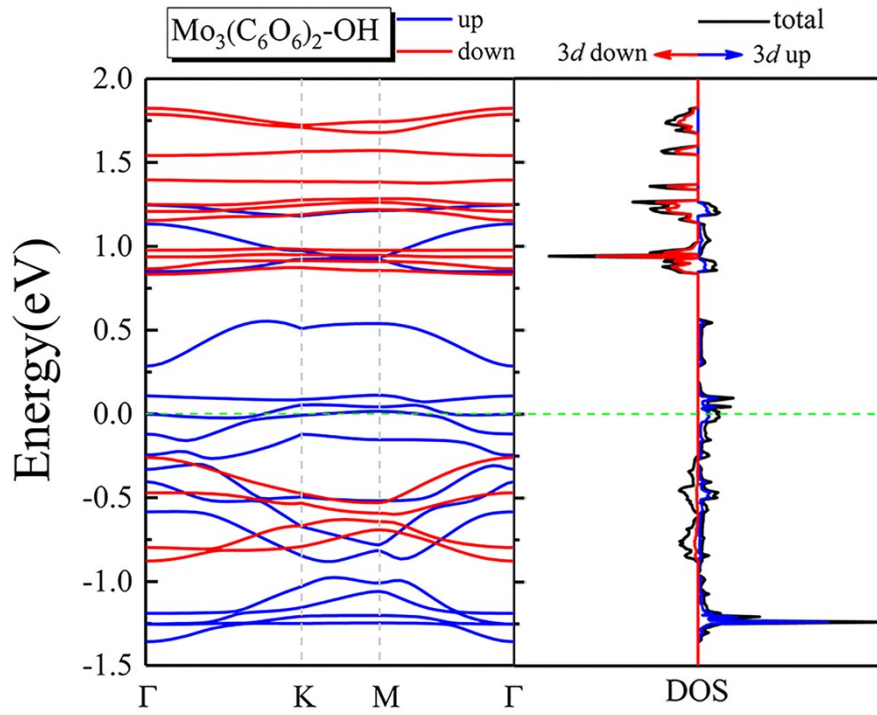


**Fig. S5** Spin-polarized band structures and density of state of  $\text{Mo}_3(\text{C}_6\text{O}_6)_2\text{-OH}$  monolayer. The blue solid line and red solid line represent the spin-up and spin-down, respectively, and the green dashed line denotes the Fermi level.